J|A|C|S
ARTICLES
Published on Web 04/02/2003

# Formation Process of Cyclodextrin Necklace−Analysis of Hydrogen Bonding on a Molecular Level

Koji Miyake,*,†,‖ Satoshi Yasuda,† Akira Harada,‡ Jun Sumaoka,§ Makoto Komiyama,§ and Hidemi Shigekawa*,†

*Contribution from the Institute of Applied Physics, 21st Century COE, University of Tsukuba, Tsukuba 305-8573, Japan, the Department of Chemistry, Graduate School of Science, Osaka University, Toyonaka, Osaka 560-0043, Japan, and the Research Center for Advanced Science and Technology, The University of Tokyo, Komaba, Tokyo 153-8904, Japan*

Received March 18, 2002; E-mail: koji-miyake@aist.go.jp, hidemi@ims.tsukuba.ac.jp

***Abstract:*** By means of scanning tunneling microscopy (STM), we succeeded for the first time in the quantitative analysis of the intramolecular conformation of a supramolecule, cyclodextrin (CyD) necklace, driven by hydrogen bonding. Contrary to the current model, based on macroscopic analyses, which indicates that all CyDs are arranged in head-to-head or tail-to-tail (secondary-secondary or primary-primary hydrogen bonding) conformation, about 20% head-to-tail (primary-secondary hydrogen bonding) conformation was found to exist in the molecule. In addition, comparing the STM results with the theoretical model of the necklace formation, the formation ratio of the tail-to-tail and head-to-tail conformations due to the strength difference between primary−primary and primary−secondary hydrogen bonds of CyDs was directly obtained, for the first time, to be 2:1.

## 1. Introduction

Understanding and optimizing the high potential of supramolecules is one of the most intriguing objectives in current nanoscience and technology[1] since supramolecules are one of the promising candidates for future molecular devices. For the further development of supramolecular materials, it is extremely important to determine their intramolecular conformations and structures and the relationship between their conformations and functions. In addition, because noncovalent bonding between component molecules strongly affects the conformational preferences and functions of a supramolecule, such as molecular recognition, catalysis, and reactivity, an understanding of the intermolecular interaction between molecules is also important. In particular, hydrogen bonding has been attracting considerable attention because of its high selectivity and directionality.

Cyclodextrin(CyD) necklace (molecular necklace) has a polyrotaxane structure; α-cyclodextrins (α-CyDs) consisting of six glucose units are threaded on a poly(ethylene glycol) (PEG) chain (Figure 1a,b). This material has been attracting considerable attention because of its high potential for use in future molecular devices, such as molecular shuttles, molecular memory, and molecular machines.[2,3]

The inclusion of a polymer chain into the cyclodextrin cavity is entropically unfavorable and is known to be promoted by the attractive interactions between the chain and the cyclodextrins such as van der Waals and hydrophobic interactions. The importance of these interactions has been clarified by previous studies.[4,5] According to the recent theoretical study,[6] the inclusion behavior becomes cooperative and CyD molecules

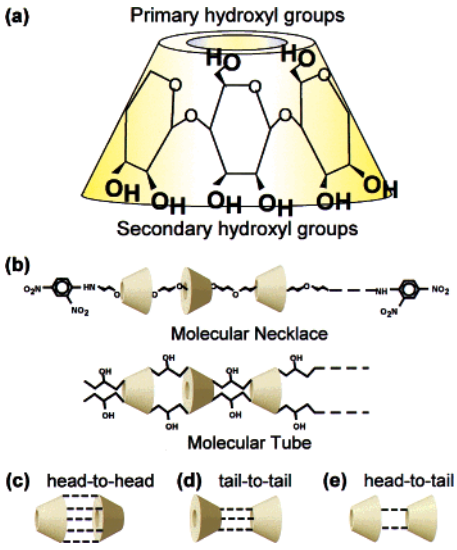


***Figure 1.*** Schematic structures of (a) cyclodextrin, (b) molecular necklace and molecular tube, and molecular conformations of (c) head-to-head, (d) tail-to-tail, and (d) head-to-tail structures.

† University of Tsukuba, 21st Century COE. http://dora.ims.tsukuba.ac.jp.
‡ Osaka University.
§ The University of Tokyo.
‖ Present address: Institute of Mechanical Systems Engineering (IMSE), National Institute of Advanced Industrial Science and Technology (AIST), 1-2-1 Namiki, Tsukuba, Ibaraki 305-8564, Japan.

(1) Lehn, J.-M. *Supramolecular Chemistry*; VCH: Weinheim, 1995.
(2) For cyclodextrin based rotaxanes: (a) Harada, A. *Acc. Chem. Res.* **2001**, *34*, 456−464. (b) Shigekawa, H.; Miyake, K.; Sumaoka, J.; Harada, A.; Komiyama, M. *J. Am. Chem. Soc.* **2000**, *122*, 5411−5412. (c) Nepogodiev, A. N.; Stoddart, J. F. *Chem. Rev.* **1998**, *98*, 1959−1976.


**10.1021/ja026224u CCC: $25.00** 

sharply include the polymer chain with increase of the attractive interaction between adjacent CyDs. Therefore, in addition to the interaction between CyDs and PEG, interaction between adjacent cyclodextrins, hydrogen-bonding, on the polymer chain plays an essential role in the inclusion behavior.

To educe and develop the high potential of the structure of polyrotaxanes, it is important to determine the conformation of the elemental molecules threaded on the molecular chains. In addition, since the conformation of the α-CyDs in a molecular necklace directly reflects the formation process, analysis of the α-CyDs conformation is important to understanding the molecular interaction from both fundamental and practical points of view.

Even when the chain PEG molecule is modified with small end groups such as methyl, dimethyl, and amino groups, they also form complexes and their yields are somewhat higher than that of unmodified PEG.[7] This indicates that the interaction between OH groups of PEG and α-CyD is not the dominant driving force for complex formation, and formation of the complex is driven by the hydrogen bonding between two α-CyDs. Namely, the hydrogen-bonding interaction plays an important role in the threading of another cyclodextrins. As a result, the hydrogen-bonding interaction between two α-CyDs is considered to determine the conformation of the α-CyDs in a molecular necklace. Therefore, in this paper, we focused on how the hydrogen-bonding interaction determines the conformation of the α-CyDs in a molecular necklace.

α-CyDs are thought to be threaded one by one from the edge of the PEG chain. Since an α-CyD has two different hydroxyl groups on the two ends of its cavity, a primary and a secondary hydroxyl group (Figure 1a), α-CyDs can have three conformations, namely, head-to-head (secondary-to-secondary; Figure 1c), tail-to-tail (primary-to-primary; Figure 1d) and head-to-tail (secondary-to-primary; Figure 1e).

The structure of the molecular necklace was characterized by nuclear magnetic resonance (NMR), ultraviolet spectroscopy, and X-ray diffraction,[8] and 100% head-to-head and tail-to-tail structure is concluded. However, the arrangement of α-CyD in the necklace is still unclear because these methods only give macroscopic and averaged information about the conformations of these supramolecules.

Scanning probe microscopy (SPM) is a leading technique for the analyses mentioned above because of its high potential and has been applied to the structural analysis of various molecules.[9,10] In fact, some molecular conformations such as chirality have been directly identified.[11,12,13] However, these were identifications of single molecules, and the determination of the intramolecular conformation of supramolecules has not yet been realized, despite its great importance.

Here, we present for the first time, by using STM, the quantitative analysis of the intramolecular conformation of a supramolecule, CyD necklace,[14] driven by the hydrogen bonding between component CyDs.

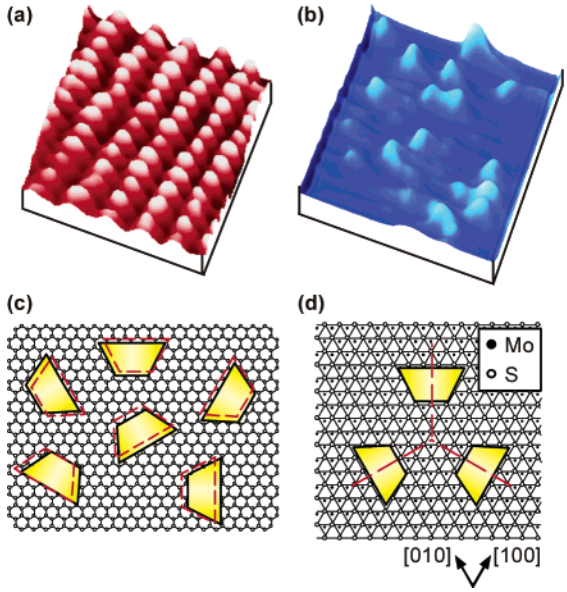


***Figure 2.*** STM images of α-CyDs on (a) highly oriented pyrolytic graphite (HOPG) (sample bias, $V_s = -30$ mV; tunneling current, $I_t = 0.6$ nA, 15 nm × 15 nm) and (b) molybdenum disulfide ($MoS_2$) substrates ($V_s = -200$ mV, $I_t = 1.0$ nA, 15 nm × 15 nm). (c) and (d) show the schematics of the lattice matching of α-CyD with HOPG and $MoS_2$, respectively.

## 2. Analysis Model: Lattice Matching Model

If the structures of supramolecules could be visualizde in real space, we could directly analyze the structures of supramolecules, such as conformation and stoichiometry. However, it is difficult to determine which side of the STM image corresponds to the head or tail of the molecule.

In our previous work, we developed an analysis method by which the conformational structure of the molecular necklace can be determined directly on a molecular level.[15] An overview of the method is given below.

**2.1. Cyclodextrins on HOPG and $MoS_2$.** Figure 2 shows typical STM images of α-CyDs on (a) HOPG and (b) $MoS_2$ substrates. Since the surfaces of these substrates are hydrophobic, it is natural for α-CyDs to be lying with their apolar outside wall on the apolar substrates. This lying conformation is more favorable than the sitting conformation where the α-CyDs

(3) For other rotaxanes: (a) Pease, A. R.; Jeppesen, J. O.; Stoddart, J. F.; Luo, Y.; Collier, C. K.; Heath, J. R. *Acc. Chem. Res.* **2001**, *34*, 433−444. (b) Ballardini, R.; Balzani, V.; Credi, A.; Gandolfi, M. T.; Venturi, M. *Acc. Chem. Res.* **2001**, *34*, 445−455. (c) Schalley, C. A.; Beizai, K.; Vögtle, F. *Acc. Chem. Res.* **2001**, *34*, 465−476. (d) Collin, J.-P.; Dietrich-Buchecker, C.; Gaviña, P.; Jimenez-Malero, M. C.; Sauvage, J.-P. *Acc. Chem. Res.* **2001**, *34*, 477−487.
(4) Ceccato, M.; Nostro, P. L.; Baglioni, P. *Langmuir* **1997**, *13*, 2436−2439.
(5) Pozuelo, J.; Mendicuti, F.; Mattice, W. L. *Macromolecules* **1997**, *30*, 3685−3690.
(6) Okumura, Y.; Ito, K.; Hayakawa. R. *Polym. Adv. Technol.* **2000**, *11*, 815−819.
(7) Harada, A.; Li, J.; Kamachi, M. *Macromolecules* **1993**, *26*, 5698−5703.
(8) Harada, A.; Li, J.; Kamachi, M. *J. Am. Chem. Soc.* **1994**, *116*, 3192−3196.
(9) Wiesendanger, R. *Scanning Probe Microscopy and Spectroscopy: Method and Application*; Cambridge University Press: New York, 1994.
(10) Bai, C. *Scanning Tunneling Microscopy and its Application*; Springer Publishing: New York, 1995.
(11) Lopinski, G. P.; Moffatt, D. J.; Wayner, D. D. M.; Wolkow, R. A. *Nature (London)* **1998**, *392*, 909−911.
(12) Fang, H.; Giancarlo, L. C.; Flynn, G. W. *J. Phys. Chem. B* **1998**, *102*, 7311−7315.
(13) Jung, T. A.; Schlitter, R. R.; Gimzewski, J. K. *Nature (London)* **1997**, *386*, 696−702.
(14) Harada, A.; Li, J.; Kamachi, M. *Nature (London)* **1992**, *356*, 325−326.
(15) Miyake, K.; Aiso, Y.; Komiyama, M.; Harada, A.; Kamachi, M.; Shigekawa, H. *Jpn. J. Appl. Phys.* **1994**, *33*, 3720−3722.
(16) Shigekawa, H.; Morizumi, T.; Komiyama, M.; Yoshimura, M.; Kawazu, A.; Saito, Y. *J. Vac. Sci. Technol. B* **1991**, *9*, 1189−1192.
(17) Yasuda, S.; Miyake, K.; Goto, Y.; Ishida, M.; Hata, K.; Fujita, M.; Yoshida, M.; Sumaoka, J.; Komiyama, M.; Shigekawa, H. *Jpn. J. Appl. Phys.* **1998**, *37*, 3844−3848.
(18) Yasuda, S.; Miyake, K.; Sumaoka, J.; Komiyama, M.; Shigekawa, H. *Jpn. J. Appl. Phys.* **1999**, *38*, 3888−3891.

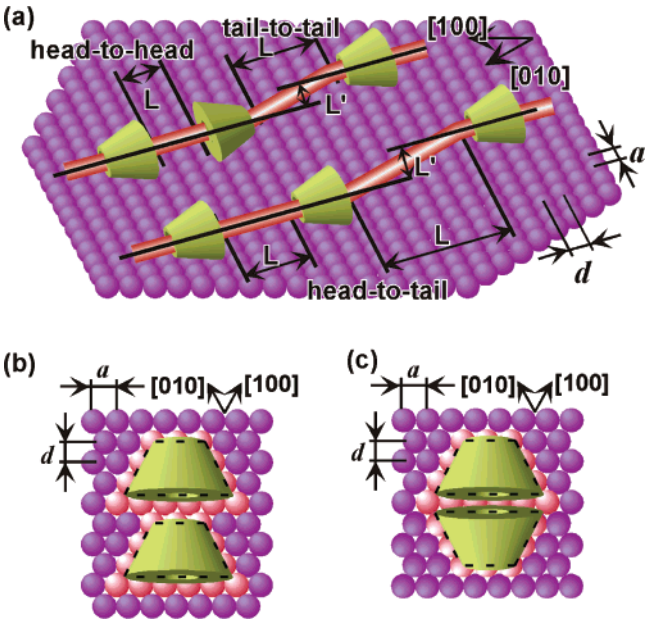


***Figure 3.*** (a) CyDs with head-to-head (tail-to-tail) and head-to-tail conformations on a $MoS_2$ surface. (b) Lattice matching between an α-CyD and S atoms on a $MoS_2$ substrate.

hydroxyl residues are contacting the apolar substrates. In the case of HOPG substrate, the interaction between CyDs and substrate is weak. Therefore, self-assembled α-CyD layers (Figure 2a) in the two-dimensional growth mode are formed by the interaction between adsorbed CyDs when the CyDs are sufficiently dense to form the monolayer.[16−18] However, it is difficult to stabilize individual CyD molecules given the low concentration of the solution. On the other hand, individual α-CyDs can be observed on the $MoS_2$ substrate stably as shown in Figure 2b, even when the concentration of α-CyD in the solution was diluted. Therefore, $MoS_2$ is appropriate for the observation of the individual α-CyD molecules.

This difference in interaction comes from the difference in lattice matching between an α-CyD molecule and the substrate. Parts c and d of Figure 2 show the schematics of α-CyD on HOPG and $MoS_2$, respectively. On HOPG substrate, there exist many equivalent physisorption sites for α-CyD. Therefore, α-CyD molecules can easily move to the neighboring stable sites on HOPG substrate. This, however, makes it difficult to observe the individual α-CyDs on HOPG substrate. On the other hand, the arrangement of sulfur atoms of the $MoS_2$ surface is commensurate with the contour of α-CyD molecules.

The commensurability between α-CyD and HOPG and $MoS_2$ is used to determine the relative orientation of adjacent α-CyDs in the molecular necklace as described below.

**2.2. Lattice Matching Model for the Analysis of the Relative Conformation of α-CyD on $MoS_2$.** By use of the lattice constants of S atoms on the $MoS_2$ surface ($d$ and $a$ shown in Figure 3a), the interstice $L$ between two adjacent α-CyDs in the [110] direction and the shift of the axis $L'$ between two adjacent α-CyDs along the $[1\bar{1}0]$ direction of $MoS_2$ can be described as

$$L = l\,d \tag{1}$$

$$L' = m(a/2) \tag{2}$$

where $d = \sim 0.27$ nm, $a = \sim 0.32$ nm, and $l$ and $m$ are integers.

α-CyD has an anisotropic shape and the positions of S atoms on the $MoS_2$ surface are shifted by $a/2$ along the [110] direction. Therefore, $L$ and $L'$ depend on the relative conformations of the two adjacent α-CyDs. For example, when two α-CyD molecules are closely located along the $[1\bar{1}0]$ direction of $MoS_2$ without shifting in the [110] direction ($m = 0$), the lattice matching conditions of the head-to-tail and head-to-head (tail-to-tail) arrangement are maintained for $l$ = even (Figure 3b) and $l$ = odd (Figure 3c), respectively.

In consideration of this lattice matching, the relative conformation of the two adjacent α-CyDs can be determined by measuring $L$ and $L'$ between two adjacent α-CyDs in STM images, namely, the arrangement of two adjacent α-CyDs is head-to-head (or tail-to-tail) and head-to-tail for $(l + m)$ being even and odd, respectively.

## 3. Experimental: STM Imaging of the Cyclodextrin Necklace

**3.1. Sample Preparation for STM Observation.** For the analysis of the conformation of the CyD necklace, STM imaging of a single molecular necklace on $MoS_2$ substrate was performed. CyD necklace molecules are insoluble in water but are soluble in 0.1 M NaOH. Therefore, these molecules were dissolved in 0.1 M NaOH, and the aqueous solution was added dropwise onto fleshly cleaved $MoS_2$ substrates. The samples were dried in air at room temperature, and then STM was performed in air at room temperature. The concentration of CyD necklace was sufficiently diluted to enable observation of an isolated chain of α-CyDs.

To confirm that the obtained STM images correspond with the molecular necklaces we used, two kinds of molecular necklaces, which have different molecular weights (MWs) of the polymer chain, were used in this experiment. One is prepared from PEG of MW = 3350, which has about 22 α-CyDs on a PEG chain (MN-3350). This corresponds to a molar ratio of 3.9, that is, more than half of the polymer chain is covered with α-CyDs. The other has about 15 α-CyDs on a PEG chain that is prepared from PEG of MW = 1450 (MN-1450). The molar ratio of ethylene glycol units to α-CyDs is 2.3. This indicates that the complex is almost stoichiometric, i.e., the CyDs are packed from end to end of a polymer chain. The number of α-CyDs in the molecular necklace and the molar ratio of ethylene glycol units to α-CyDs were estimated from the results of NMR measurement.[19]

**3.2. STM Images of Cyclodextrin Necklace.** Figure 4 shows the STM images of the molecular necklaces, in which the molar ratios of ethylene glycol units to α-CyDs are (a) 3.9 (MN-3350) and (b) 2.3 (MN-1450), respectively. The molar ratio of PEG to α-CyDs was determined by the $^1$H NMR.[19] In both cases, an $MoS_2$ substrate was used. The molecular necklaces were stably observed during STM scan. Regularly aligned α-CyDs were clearly observed as shown in Figure 4. In the case of MN-3350, α-CyDs were observed separately in their linear forms and an interstice between two adjacent α-CyDs on the PEG chain was observed, as shown in Figure 4a. On the other hand, closely packed α-CyD molecules were observed in the case of MN-1450, as shown in Figure 4b. The observed structures were in good agreement with the molecular structures previously proposed, in which α-CyDs were threaded on a PEG chain. In addition, the molar ratios of MN-3350 and MN-1450 estimated from STM images were about 4 and 2, which also agree well with the results of NMR measurement.[19]

## 4. Determination of the Relative Orientation of Adjacent α-CyDs

**4.1. Measurement Procedure.** The structure and molar ratio of the CyD necklace were visualized in real space at the

(19) Harada, A.; Li, J.; Nakamitsu, T.; Kamachi, M. *J. Org. Chem.* **1993**, *58*, 7524−7528.

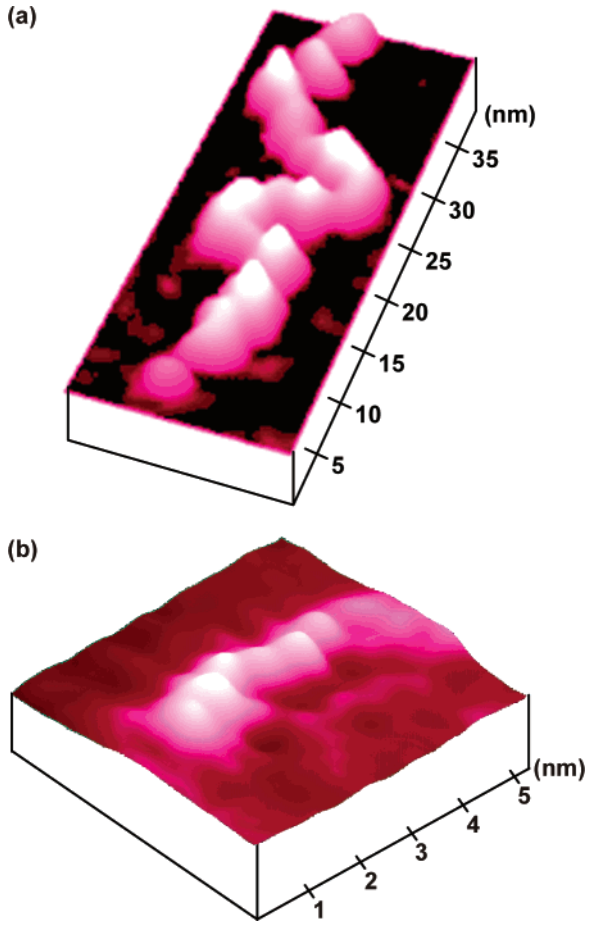


***Figure 4.*** STM images of molecular necklaces, where the molar ratio of ethylene glycol units to α-CyDs is (a) 3.9 (MN-3350) ($V_s = -250$ mV, $I_t = 2.0$ nA) and (b) 2.3 (MN-1450) ($V_s = 200$ mV, $I_t = 0.9$ nA), respectively.

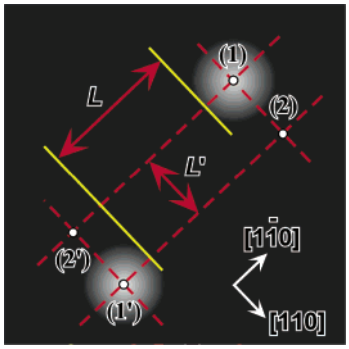


***Figure 5.*** Determination procedure of the relative orientation of adjacent α-CyDs.

molecular level by using STM. However, as mentioned in section 3, since the primary and secondary hydroxyl groups cannot be discriminated in the STM image, it is difficult to determine the conformation of adjacent CyDs in the molecular necklace. The conformations are determined by using the lattice matching model.

We determined the relative orientations of adjacent α-CyDs from STM images by the following procedures (Figure 5).

1. Highest positions of the two α-CyD molecules were determined as the reference points ((1) and (1′)).

2. Four straight lines passing through the two reference points of the molecules were drawn along the [110] and [1$\bar{1}$0] direction

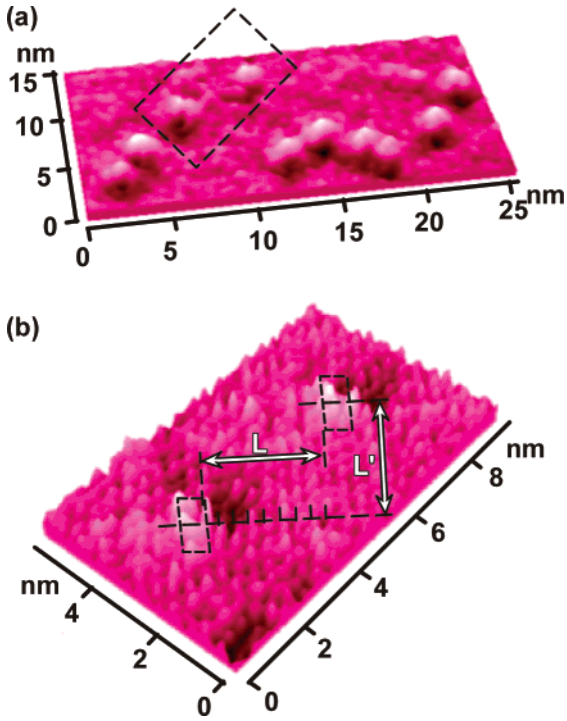


***Figure 6.*** STM image ($V_s = -200$ mV, $I_t = 1.0$ nA) of a molecular necklace (a) and its magnification of the squared part in (a) with the contrast focused on the $MoS_2$ lattice (b) ($V_s = -130$ mV, $I_t = 1.0$ nA).

(four red dotted lines). And the two intersections were marked ((2) and (2′)).

3. The values $L'$ can be determined by measuring the distance, (1)−(2) or (1′)−(2′).

4. On the other hand, in the case of $L$, the rim-to-rim distance is necessary. Therefore, the size of a α-CyD molecule (=0.70 nm) was subtracted from the measured distance of (1)−(2′) or (1′)−(2).

5. From eqs 1 and 2, the integers $l$ and $m$ were obtained by dividing $L$ and $L'$ by $d$ (=0.27 nm) and $a/2$ (=0.16 nm), respectively.

6. Then, when $(l + m)$ became odd (even), the arrangement of the two adjacent α-CyDs was determined as head-to-head or tail-to-tail (head-to-tail).

**4.2. Example of Conformational Analysis and Statistics.** Figure 6a is a STM image of a molecular necklace. A magnification of the square part in Figure 6a is shown in Figure 6b with the contrast focused on the $MoS_2$ lattice. Following the procedure described in 4.1, the values $L$ and $L'$ were measured as 2.20 and 2.75 nm, respectively. And $l$ and $m$ were determined as 8 ($L/d = 2.20/0.27 \sim 8.15$) and 17 ($L'/(a/2) = 2.75/(0.32/2) \sim 17.19$), respectively. Therefore, $(l + m)$ is 25, namely, odd, in this case, and indicates that the conformation of the two adjacent α-CyD molecules is head-to-tail

This result also indicates that there must exist eight sulfur rows along the [110] direction between adjacent CyD molecules. Here, since contrast is focused on the $MoS_2$ lattice, the existence of the eight sulfur rows can actually be observed between CyD molecules.

We measured $L$ and $L'$ for about 100 CyD molecular pairs, and the results are summarized in Figure 7a. The head-to-head and head-to-tail conformations are represented by ◆ and ■, respectively. Figure 7b and c show the histograms of the

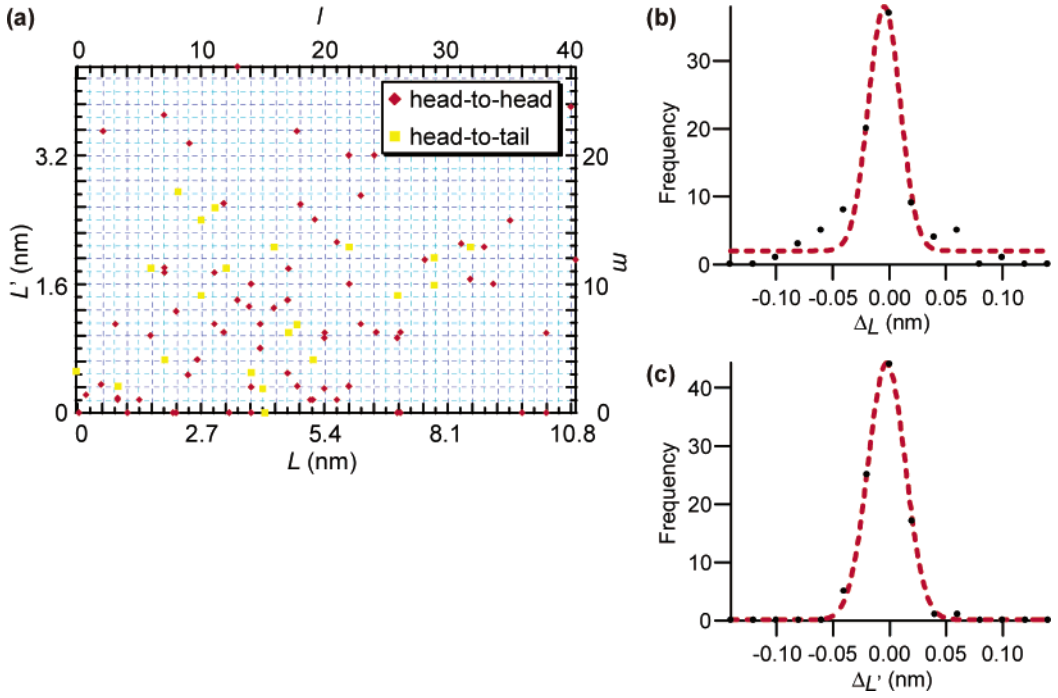


***Figure 7.*** (a) Experimentally obtained values of $L'$ and $L'$. (b) (c) Histograms of the difference between the measured values of $L$ or $L'$ and the ideal integer multiples of the elementary lattice constants of the axes, respectively.

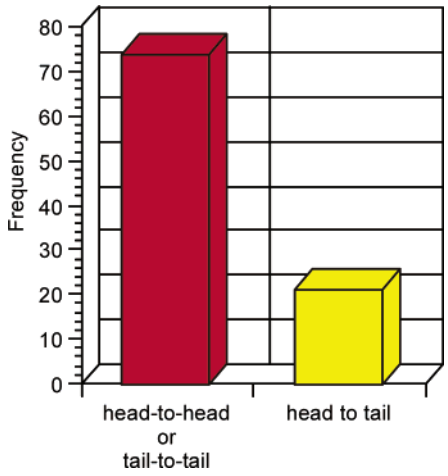


***Figure 8.*** Number of head-to-head (or tail-to-tail) and head-to-tail conformations determined from STM measurements.

difference between the measured values of $L$ or $L'$ and the ideal integer multiples of the elementary lattice constants of the axes, respectively. As shown in the figures, $\delta L$ and $\delta L'$ are within 0.05 nm, resulting in the differences from the integers as $\delta l < \sim 0.2$ and $\delta m < \sim 0.3$, respectively. These values are sufficient to determine the relative orientations by using our model.

**4.3. Results of the Relative Orientation of Adjacent α-CyDs.** Figure 8 summarizes the numbers of head-to-head (or tail-to-tail) and head-to-tail conformations determined from STM measurements. As shown in Figure 8, about 80% of the conformation is head-to-head or tail-to-tail, contrary to the model proposed on the basis of the macroscopic analyses. Namely, 20% head-to-tail conformations were found microscopically, for the first time, to exist.

## 5. Analysis of Formation Process

**5.1. Formation Process and Observed Structures.** Now let us examine the inclusion process in detail. From comparison between a theoretical model with the result shown in Figure 8, the formation ratio of the tail-to-tail and head-to-tail conformations is analyzed. CyDs are included from the left side here, following the schematic model shown in Figure 9. If the secondary−secondary interaction is sufficiently strong compared to the secondary−primary interaction, only the secondary−secondary (head-to-head) conformation is realized when the left end of the threaded CyDs is the secondary side (Figure 9a). Therefore, the primary−secondary (head-to-tail) conformation is introduced only when the left end of the threaded CyDs is the primary side (Figure 9c). In this case, the primary−secondary (head-to-tail) conformation has a single orientation; the primary hydroxyl of the head-to-tail unit (tail side) is oriented toward the left side, as indicated by solid triangles in Figure 9d. In fact, the experimentally observed head-to-tail CyD units are in the expected single orientation extending over ~10 CyDs from each end (approximately the center from either edge of a molecular necklace).

**5.2. Model for the Analysis.** To reproduce the experimental results in Figure 8 by calculation, we adopt the following conditions. When the end of the threaded CyD molecules is the secondary side, it forms a hydrogen bond with the following CyD by secondary−secondary (head-to-head) conformation (Figure 9a). On the other hand, when the last end is the primary side, both tail-to-tail and head-to-tail conformations are realized.

Because CyDs are included from the left side in this model, hydroxyl groups on the right-hand side form hydrogen bonds with an included CyD at first. Therefore, we focused on the conformation of the right-hand side of each CyD. When the conformations of the right-hand side of CyD are head-to-head, tail-to-tail, and head-to-tail, they are called h-h, t-t, and h-t, respectively. On the basis of this assumption, the total number of CyD molecules in a single CyD necklace ($N_{total}$) can be represented by

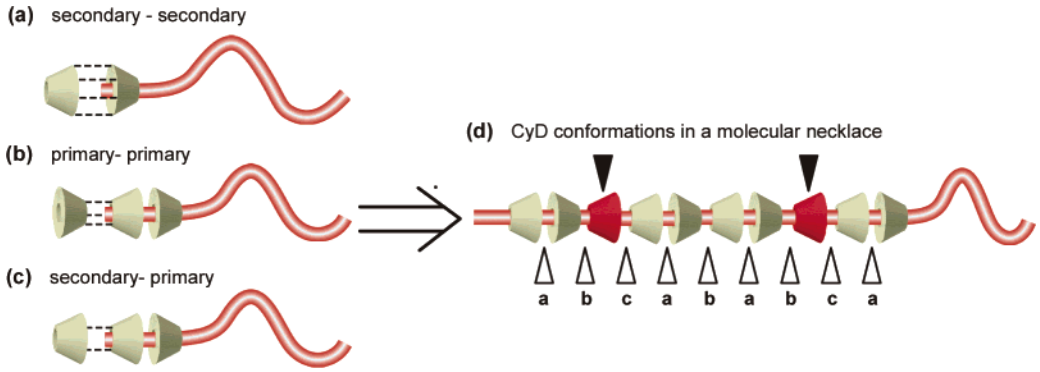


***Figure 9.*** Three different conformations appearing in the inclusion process of a molecular necklace formation: (a) secondary−secondary, (b) primary−primary, and (c) secondary−primary and (d) CyD conformations in a molecular necklace.

$$N_{\text{total}} = N_{\text{h-h}} + N_{\text{t-t}} + N_{\text{h-t}} + 1 \quad (3)$$

where $N_{\text{h-h}}$, $N_{\text{t-t}}$, and $N_{\text{h-t}}$ are the numbers of h-h, t-t, and h-t CyDs; i.e., they correspond to the numbers of head-to-head, tail-to-tail, and head-to-tail conformations, respectively. Here the term +1 corresponds to the first included CyD molecule in the molecular necklace.

The ratio of the head-to-tail conformation $r$ can be expressed as

$$r = N_{\text{h-t}}/(N_{\text{h-h}} + N_{\text{t-t}} + N_{\text{h-t}}) \quad (4)$$

Here, supposing that the head-to-tail conformation is introduced with a probability of $1/n$, it can be written as

$$1/n = N_{\text{h-t}}/(N_{\text{t-t}} + N_{\text{h-t}}) \quad (5)$$

When $N_{\text{total}}$ is constant, $N_{\text{h-h}}$ and $N_{\text{t-t}}$ have the relationship

$$N_{\text{h-h}} = N_{\text{t-t}} + c \quad (c = \pm 1 \text{ or } 0) \quad (6)$$

When the left end of the CyD included first is the secondary side as shown in Figure 10a, the value of $c$ becomes 0 or 1 for the orientation of the last CyD molecule to be the same as (Figure 10a) or opposite to (Figure 10b) the first one, respectively. On the other hand, when the left end of the CyD included first is the primary side as shown in Figure 10c, the value of $c$ becomes 0 or −1 for the orientation of the last CyD molecule to be the same as (Figure 10c) or opposite to (Figure 10d) the first one, respectively.

From eqs 3, 4, 5, and 6, $r$ is expressed as

$$r = \frac{1}{2n-1}\left(1 - \frac{c}{N_{\text{total}} - 1}\right) \quad (7)$$

Since CyD molecules are randomly included, the average value of $c$ becomes 0. Therefore, the average value of $r$ becomes

$$\bar{r} = \frac{1}{2n-1} \quad (8)$$

**5.3. Results of Analysis.** Using eq 8, $\bar{r}$ becomes 0.20 for $n = 3$, which corresponds to the experimental result (~0.2, Figure 8).

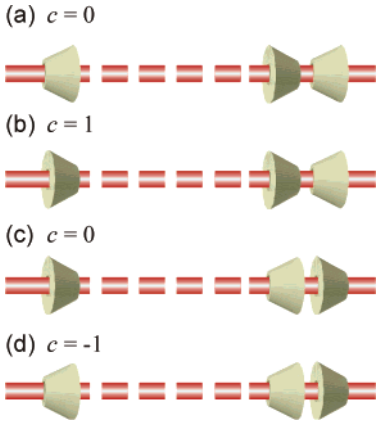


***Figure 10.*** Four conformations of the CyDs in a molecular necklace and the corresponding values of $c$ appearing in eq 6: (a) and (c) CyD molecules with both ends having the same orientation ($c = 0$). (b) CyD molecules with both ends having the tail-to-tail conformation ($c = 1$). (d) CyD molecules with both ends having the head-to-head conformation ($c = -1$).

This result indicates that the primary−secondary (head-to-tail) hydrogen bonding is 2 times more difficult to realize than the primary-primary (head-to-head) configuration during the inclusion process. This is the first quantitative determination of the hydrogen bonding between CyDs during the supramolecular formation process.

## 6. Conclusion

The intramolecular structure of the molecular necklace was analyzed on a molecular level for the first time. The role of hydrogen bonding in the formation process was confirmed. Contrary to the current model that is based on macroscopic analyses, indicating that all CyDs are arranged in head-to-head and tail-to-tail conformations, about 20% head-to-tail conformation was found to exist in the molecule. From the analysis of this result with a stochastic model, the formation ratio of the tail-to-tail and head-to-tail conformations due to the primary−primary and primary−secondary hydrogen bonding of CyDs, was quantitatively evaluated, for the first time, to be 2:1.

**Acknowledgment.** This work was supported by a Grant-in-Aid for Scientific Research from the Ministry of Education, Culture, Sports, Science and Technology, Japan.

JA026224U